J Gastroenterol (2017) 52:965–976
DOI 10.1007/s00535-016-1304-z

The Japanese Society of Gastroenterology

ORIGINAL ARTICLE—LIVER, PANCREAS, AND BILIARY TRACT

Hepatic vagus nerve regulates Kupffer cell activation via α7 nicotinic acetylcholine receptor in nonalcoholic steatohepatitis

Takahiro Nishio[1] · Kojiro Taura[1] · Keiko Iwaisako[1,2] · Yukinori Koyama[1] · Kazutaka Tanabe[1] · Gen Yamamoto[1] · Yukihiro Okuda[1] · Yoshinobu Ikeno[1] · Kenji Yoshino[1] · Yosuke Kasai[1] · Masayuki Okuno[1] · Satoru Seo[1] · Takaki Sakurai[3] · Masataka Asagiri[4] · Etsuro Hatano[1,5] · Shinji Uemoto[1]

Received: 6 September 2016 / Accepted: 22 December 2016 / Published online: 2 January 2017

Abstract

Background Nonalcoholic fatty liver disease ranges from simple steatosis to nonalcoholic steatohepatitis (NASH). Kupffer cells play a central role in promoting hepatic inflammation, which leads to the development of NASH. We investigated the anti-inflammatory effect of hepatic vagus-mediated stimulation of the α7 nicotinic acetylcholine receptor (α7nAChR) on Kupffer cells in NASH pathogenesis.

Methods Wild-type (WT) mice undergoing hepatic vagotomy (HV) were fed a methionine- and choline-deficient (MCD) diet for 1 week. α7nAChR knockout (α7KO) chimeric mice were generated by transplanting α7KO bone marrow cells into irradiated and Kupffer cell-deleted WT recipients. Kupffer cells were isolated from WT mice and treated with α7nAChR agonist under stimulation by lipopolysaccharide and/or palmitic acid.

Results HV aggravated MCD diet-induced NASH in both steatosis and inflammation. The hepatic inflammatory response, including the upregulation of tumor necrosis factor alpha (TNFα), interleukin (IL)-12, and monocyte chemoattractant protein 1 (MCP-1), was accelerated in HV mice, accompanied by the downregulation of PPARα pathway genes. Kupffer cells were highly activated via the phosphorylation and nuclear translocation of nuclear factor-kappa B (NF-κB) in MCD diet-fed HV mice. The α7nAchR agonist suppressed the inflammatory response of primary Kupffer cells induced by lipopolysaccharide and palmitic acid by attenuating the NF-κB cascade. α7KO chimeric mice fed an MCD diet for 1 week developed advanced NASH with highly activated Kupffer cells. The hepatic expression of TNFα, IL-12, and MCP-1 was upregulated in α7KO chimeric mice, accompanied by abnormal lipid metabolism.

Conclusions Hepatic vagus activity regulates the inflammatory response of Kupffer cells via α7nAChR in NASH development.

Keywords NASH · NAFLD · Fatty liver disease · α7nAChR · Vagotomy

Abbreviations

NAFLD	Nonalcoholic fatty liver disease
NASH	Nonalcoholic steatohepatitis
TLR	Toll-like receptor
IL	Interleukin
TNFα	Tumor necrosis factor alpha
MCP-1	Monocyte chemoattractant protein 1
α7nAChR	α7 nicotinic acetylcholine receptor

Electronic supplementary material The online version of this article (doi:10.1007/s00535-016-1304-z) contains supplementary material, which is available to authorized users.

✉ Kojiro Taura
ktaura@kuhp.kyoto-u.ac.jp

1 Department of Surgery, Graduate School of Medicine, Kyoto University, 54 Kawahara-cho, Shogoin, Sakyo-ku, Kyoto, Japan

2 Department of Target Therapy Oncology, Graduate School of Medicine, Kyoto University, Kyoto, Japan

3 Department of Diagnostic Pathology, Graduate School of Medicine, Kyoto University, Kyoto, Japan

4 Innovation Center for Immunoregulation and Therapeutics, Graduate School of Medicine, Kyoto University, Kyoto, Japan

5 Department of Surgery, Hyogo College of Medicine, Hyogo, Japan

STAT3	Signal transducer and activator of transcription 3
NF-κB	Nuclear factor-kappa B
MCD	Methionine- and choline-deficient
WT	Wild type
α7KO	α7nAChR knockout
HV	Hepatic vagotomy
CT	Control
BM	Bone marrow
GAPDH	Glyceraldehyde 3-phosphate dehydrogenase
LPS	Lipopolysaccharide
PPARα	Peroxisome proliferator-activated receptor alpha
AOX	Acyl-CoA oxidase
L-FABP	Liver-type fatty acid binding protein
SREBF-1c	Sterol regulatory element binding factor 1c
FAS	Fatty acid synthase
G6pc	Glucose 6-phosphatase
PEPCK	Phosphoenolpyruvate carboxykinase 1
GFP	Green fluorescent protein

Introduction

Nonalcoholic fatty liver disease (NAFLD), a hepatic consequence of metabolic syndrome, has become a common cause of chronic liver diseases worldwide as a result of an epidemic rise in obesity [1–3]. The disease spectrum of NAFLD ranges from simple steatosis to nonalcoholic steatohepatitis (NASH), which is characterized by steatosis with progressive inflammation and fibrosis, and eventually leads to liver cirrhosis and the development of hepatocellular carcinoma [4, 5]. The "two-hit" model [6], which has been proposed as a potential mechanism of NASH pathogenesis for more than a decade, suggested that the first hit of steatosis and the second hit, which includes oxidative stress, innate immunity, adipocytokines, or gut-derived endotoxins, are required to progress from simple steatosis to NASH. On the other hand, recent studies have indicated that inflammation resulting from multiple parallel hits also precedes steatosis in NASH, as inflammatory events may lead to subsequent steatosis [7–9]. Elucidating the mechanism that regulates the initiation of the inflammatory response is essential in determining preventive and therapeutic approaches for treating patients with NASH.

The activation of the hepatic innate immune system is associated with the inflammatory response in NASH pathogenesis [7, 10]. Kupffer cells, which are liver-resident macrophages, play a central role in promoting hepatic inflammation by innate immune responses via Toll-like receptor (TLR) signaling [11–15]. Activated Kupffer cells induce liver injury by producing pro-inflammatory cytokines, e.g., interleukin (IL)-1β, IL-12, tumor necrosis factor alpha (TNFα), and monocyte chemoattractant protein 1 (MCP-1) [15–19]. Regulating Kupffer cell activity might be a key approach for suppressing NASH progression.

Efferent vagus nerve-mediated cholinergic signaling is known to play an important role in regulating innate immune responses and inflammation, and this signaling has been defined as the cholinergic anti-inflammatory pathway, the efferent arm of inflammatory reflux [20–22]. The α7 nicotinic acetylcholine receptor (α7nAChR), which is expressed in immune cells such as macrophages and monocytes, is involved in mediating the inhibition of pro-inflammatory cytokine production via intracellular signaling pathways [23]. The pathways downstream of α7nAChR upon cholinergic stimulation include the activation of Janus kinase 2 and the subsequent phosphorylation of signal transducer and activator of transcription 3 (STAT3), as well as the suppression of nuclear factor-kappa B (NF-κB) nuclear translocation [24–27].

Several studies have reported that vagus nerve-mediated cholinergic activation has protective effects against obesity-related inflammation and other metabolic complications [28–30]. NASH, a hepatic result of chronic inflammation based on metabolic disorder, is likely to be affected by vagus nerve activity; however, the specific effect of hepatic vagus signaling on the modulation of inflammatory responses in NASH pathogenesis remains unclear.

In the present study, we sought to elucidate the role of the hepatic vagus nerve in the regulation of Kupffer cell-mediated inflammatory responses via α7nAChR stimulation in the setting of NASH. We specifically focused on the early developmental phase by using a methionine- and choline-deficient (MCD) dietary experimental model.

Methods

Animal handling, surgical procedures, and diets

Wild-type (WT) C57BL/6 mice, C57BL/6-Tg (CAG-EGFP) mice, and α7nAChR-/- (α7KO) mice on the C57BL/6 background were obtained from Japan SLC (Shizuoka, Japan), CLEA Japan (Tokyo, Japan), and the Jackson Laboratory (Bar Harbor, ME, USA). The mice were housed under a 12-hour light–dark cycle with free access to food and water. Animals received humane care, and all procedures were performed according to protocols approved by the animal research committee of Kyoto University.

Male WT mice (12 weeks old) were subjected to hepatic vagus denervation. A selective hepatic vagotomy (HV) was performed as previously described [31]. Briefly, a laparotomy was made at the midline, the fibrous attachment of the gastrohepatic ligament was dissected, and the stomach was gently pulled down. The ventral subdiaphragmatic vagus trunk was exposed along the descending esophagus. The common hepatic branch of the vagus nerve, which leaves the trunk and travels towards the hepatic portal region, was completely transected with ligation of each margin. Sham-operated mice underwent a laparotomy without the transection of the common hepatic vagus branch.

One week after surgery, the mice were fed a control (CT) or MCD diet (Research Diets #A07080109, 35 kcal% fat) for 1 or 8 weeks. The mice were subjected to fasting for 12 h before sacrifice, and samples were collected.

Generating chimeric mice

To generate chimeric mice, WT recipients (male, 6 weeks old) were intraperitoneally injected with 200 μL of liposomal clodronate (FormuMax Scientific, Sunnyvale, CA, USA) to deplete Kupffer cells 24 h before bone marrow (BM) transplantation. BM cells (2×10^7 cells) obtained from WT, α7KO, or C57BL/6-Tg(CAG-EGFP) mice were transplanted by intravenous injection into lethally irradiated recipient mice (10 Gy). MCD diet feeding started 8 weeks after BM transplantation.

Histological examination

Formalin-fixed specimens were embedded in paraffin, sectioned at a thickness of 4 μm, and mounted on silanized glass slides. The paraffin-embedded sections were stained with hematoxylin and eosin, toluidine blue (Wako, Osaka, Japan), or Sirius Red (Wako). For Nile Red (Lonza, Basel, Switzerland) staining, the specimens were fixed in 4% paraformaldehyde, embedded in optimal cutting temperature compound (Sakura, Tokyo, Japan), and sectioned at a thickness of 4 μm. For immunohistochemical staining, the specimens fixed in 4% paraformaldehyde and embedded in optimal cutting temperature compound were also sectioned at a thickness of 4 μm. Antigen retrieval was performed by incubation in citric acid buffer at 90 °C for 20 min. After blocking, the sections were incubated with a primary antibody against F4/80 (Cat. No. 14-4801, eBioscience, San Diego, CA, USA), phospho-NF-κB p65 (Cat. No. ab106129, Abcam, Cambridge, MA), or α7nAChR (Cat. No. ANC-007, Alomone Labs, Jerusalem, Israel) at 1:200 dilution overnight at 4 °C, followed by incubation with a corresponding secondary antibody at room temperature for 1 h. Positively stained areas or cell counts were measured in 10 fields (at ×100 magnification) per specimen using the National Institutes of Health ImageJ image analysis software [32]. The NAFLD activity score was determined by a pathologist (T.S.) in a blinded manner according to published criteria [33].

Quantitative real-time polymerase chain reaction

Total RNA was extracted from liver tissue or cell samples using TRIzol reagent (Life Technologies, Carlsbad, CA, USA) and the RNeasy Mini Kit with on-column DNA digestion (Qiagen, Valencia, CA, USA). The extracted RNA was reverse transcribed to complementary DNA using the Omniscript RT kit (Qiagen). The quantitative real-time polymerase chain reaction was performed with a KAPA SYBR FAST qPCR Kit (NIPPON Genetics, Tokyo, Japan) using a StepOnePlus system (Applied Biosystems, Foster City, CA, USA). Glyceraldehyde 3-phosphate dehydrogenase (GAPDH) and 18S rRNA were used as internal controls. Data normalized to 18S are shown. The primer sequences are summarized in Table S1.

Measurement of tissue triglyceride and acetylcholine content

Hepatic triglycerides were extracted using the Folch method [34], and their levels were measured using Triglyceride E (Wako). Acetylcholine was isolated from the liver or spleen, and its concentration was measured using an Amlite™ Fluorimetric Acetylcholine Assay Kit (AAT Bioquest, Sunnyvale, CA, USA). The resultant values were normalized to the tissue protein concentrations.

Western blot

Western blot analysis was conducted as previously described [35]. Blots were incubated with primary antibody against α7nAChR (Cat. No. ab23832, Abcam), phospho-p65 (Cat. No. ab106129, Abcam), p65 (Cat. No. ab7970, Abcam), phospho-STAT3 (Cat. No. ab30647, Abcam), STAT3 (Cat. No. ab68153, Abcam), or GAPDH (Cat. No. sc-25778, Santa Cruz Biotechnology, Dallas, TX, USA) at 1:1000 dilutions. The band intensities were quantified using ImageJ.

Serum biochemistry

The levels of aspartate aminotransferase, alanine aminotransferase, triglyceride, total cholesterol, and glucose were measured in serum samples obtained after 12 h of fasting following CT or MCD diet feeding.

Cell culture and treatment

Kupffer cells were isolated via a two-step collagenase-pronase perfusion of mouse livers followed by 15% Nycodenz (Nycomed Pharm, Oslo, Norway) two-layer discontinuous density gradient centrifugation as previously described [14]. The cell fraction was purified using magnetic antibody cell sorting (MACS; Miltenyi Biotec, Bergisch Gladbach, Germany) with CD11b-conjugated microbeads (Miltenyi Biotec). Isolated cells were cultured for 16 h in Dulbecco's modified eagle's medium containing 10% fetal bovine serum and antibiotics prior to stimulation by reagents. Lipopolysaccharide (LPS) (1 ng/mL; Sigma-Aldrich, St. Louis, MO, USA) and/or palmitic acid (400 μM; Sigma-Aldrich) were added to the culture medium, and the cells were stimulated for 6 h. The cells were pre-treated with vehicle or α7nAChR agonist (PNU 282987; Abcam) 30 min prior to the administration of LPS and/or palmitic acid.

Statistical analysis

Data are presented as the mean ± SD. Differences between groups were compared using Student's *t* test or a one-way analysis of variance followed by the Tukey–Kramer test. $p < 0.05$ was considered significant. The JMP Pro 11 (SAS institute, Cary, NC, USA) software was used for all statistical analyses.

Results

Hepatic vagus nerve denervation aggravates MCD diet-induced NASH

WT mice were subjected to HV or a sham operation and were fed an MCD diet for 1 week. In the HV procedure, the common hepatic branch of the vagus nerve was transected, which was histologically confirmed in the resected tissue specimen (Fig. S1a). The hepatic acetylcholine content was significantly attenuated after HV, whereas the acetylcholine levels in the spleen were unaffected (Fig. S1b). Mice fed an MCD diet for 1 week developed early-stage steatohepatitis with mild inflammation (Fig. 1a). In this short time period, the attenuation of hepatic acetylcholine levels after HV was maintained in both MCD diet-fed and CT diet-fed mice (Fig. S1c). HV enhanced MCD diet-induced steatohepatitis, as demonstrated by aggravated histological findings of both steatosis and lobular inflammation (Fig. 1a), whereas it did not affect the normal livers of CT diet-fed mice. In the MCD diet-fed mice, hepatic lipid accumulation was significantly increased by HV, as indicated by the lipid staining of liver tissue and quantification of hepatic triglyceride content (Fig. 1b, c). The increased transaminase levels suggested that HV promoted NASH-induced liver damage (Fig. 1d). Weight loss and low total serum cholesterol levels were observed in MCD diet-fed mice, and these changes are features of the MCD dietary model due to the reduction of hepatic lipid secretion. HV did not affect body weight, adipose tissue weight, or serum lipid levels (Table 1).

Hepatic vagus denervation promotes NASH-associated inflammatory responses and abnormal lipid metabolism

Based on the aggravation of early-stage NASH by HV, we assessed the regulatory effect of the hepatic vagus nerve on inflammatory responses and lipid metabolism. The hepatic expression of pro-inflammatory cytokines associated with NASH pathogenesis, including TNFα and IL-12, was significantly increased in MCD diet-fed mice that had undergone HV. MCP-1, a key chemokine responsible for macrophage infiltration, was also upregulated. The levels of IL-1β and IL-6 expression were not affected by HV (Fig. 2a).

Among lipid metabolism regulators, the expression of peroxisome proliferator-activated receptor alpha (PPARα)-pathway genes was significantly decreased by HV in MCD diet-fed mice, including PPARα and its downstream targets acyl-CoA oxidase (AOX) and liver-type fatty acid binding protein (L-FABP), which are key regulators of β-oxidation. The expression of genes involved in fatty acid synthesis, including sterol regulatory element binding factor 1c (SREBF-1c) and fatty acid synthase (FAS), were unaffected (Fig. 2b). Regarding glucose metabolism, the hepatic expression of gluconeogenic genes, including glucose 6-phosphatase (G6pc) and phosphoenolpyruvate carboxykinase 1 (PEPCK), was decreased in the MCD diet-fed mice, and it was significantly downregulated by HV, whereas the serum glucose level was not affected (Fig. S2). Conversely, the hepatic expression of G6pc was increased in the HV mice fed a control diet, indicating that attenuating the vagus-mediated suppressive effect on gluconeogenesis may upregulate hepatic gluconeogenetic gene expression in the normal liver [36].

Because liver fibrosis is a consequence of advanced NASH, we further investigated the influence of HV on NASH-induced liver fibrosis using mice fed an MCD diet for 8 weeks. These mice developed mild liver fibrosis but did not form septa or exhibit bridging (Fig. S3a). HV did not significantly affect the hepatic expression of genes involved in inflammation, fibrosis, or lipid metabolism (Fig. S3b, c, and d). Notably, the chronic choline-deficient status of MCD dietary intake resulted in a slow decrease in hepatic acetylcholine levels, which led to the attenuation of the HV

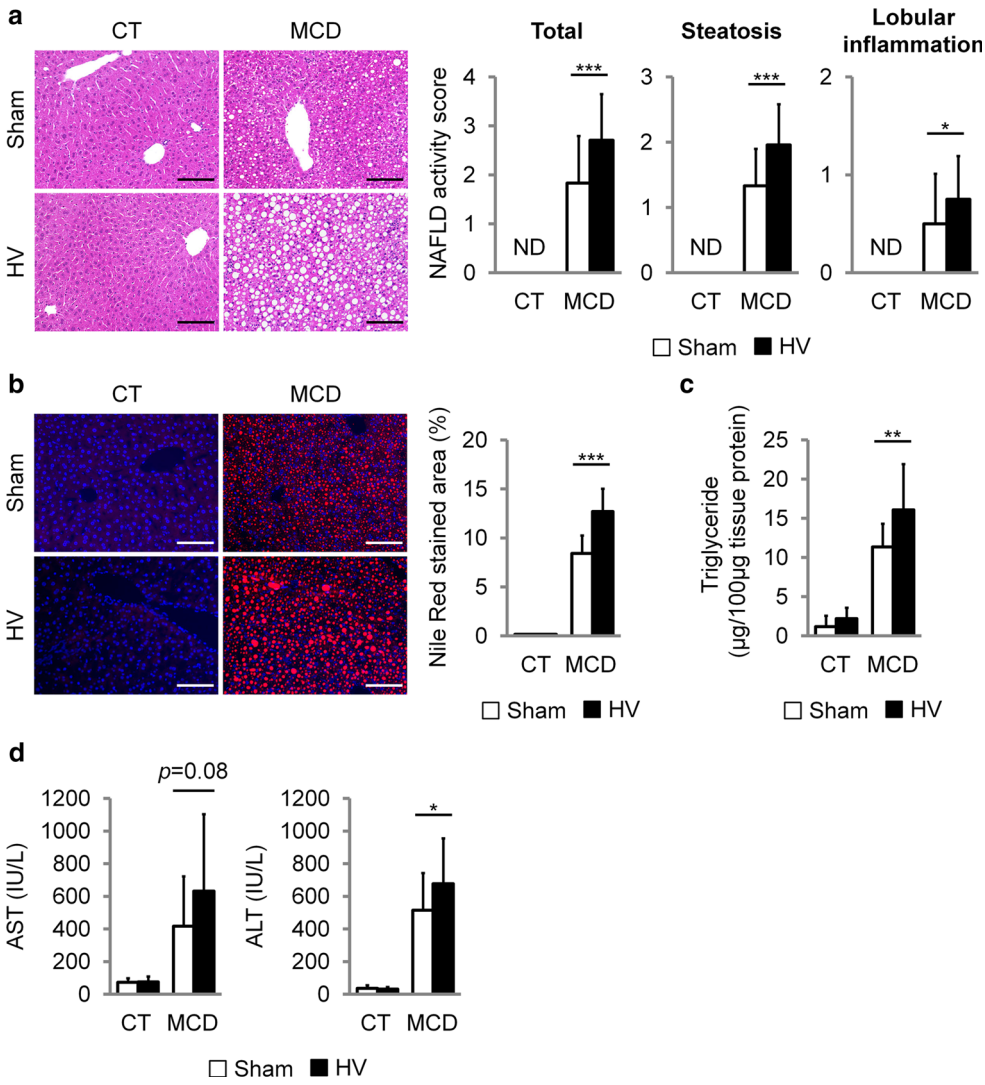

Fig. 1 Hepatic vagus denervation aggravates MCD diet-induced NASH. WT mice underwent a sham operation or HV and were fed a CT or MCD diet for 1 week. **a** *Left* Hematoxylin and eosin staining of liver sections. *Right* NAFLD activity score. **b** *Left* Nile Red staining of liver sections. *Right* Quantification of Nile Red-stained area. Original magnification ×100; scale bars, 100 μm. **c** Hepatic triglyceride content. **d** Serum aspartate aminotransferase (AST) and alanine aminotransferase (ALT) levels. $n = 6$ per CT-diet group; $n = 12$ per MCD-diet group. Data represent the mean ± SD. $^{*}p < 0.05$; $^{**}p < 0.01$; $^{***}p < 0.001$. *ND* not detected

Table 1 Body, liver, and adipose tissue weight and serum lipid levels after MCD diet feeding

	CT diet		MCD diet	
	Sham ($N = 6$)	HV ($N = 6$)	Sham ($N = 12$)	HV ($N = 12$)
BW change (%)	2.9 ± 3.3	1.1 ± 2.3	−12.0*[a] ± 2.3	−13.2*[a] ± 2.6
Liver weight (% BW)	3.9 ± 0.6	4.1 ± 0.5	4.3 ± 0.3	4.5 ± 0.4
SAT weight (% BW)	0.84 ± 0.27	0.92 ± 0.12	0.91 ± 0.30	0.90 ± 0.15
VAT weight (% BW)	0.86 ± 0.36	1.00 ± 0.23	0.92 ± 0.28	0.94 ± 0.25
Serum TG (mg/dL)	28.8 ± 7.1	26.3 ± 11.3	21.8 ± 4.2	27.1 ± 12.3
Serum TC (mg/dL)	85.1 ± 10.9	82.5 ± 13.4	45.2 *[a] ± 8.8	38.8*[a] ± 6.8

Values are presented as the mean ± SD

MCD methionine- and choline- deficient, *CT* control, *HV* hepatic vagotomy, *BW* body weight, *SAT* subcutaneous adipose tissue, *VAT* visceral adipose tissue, *TG* triglyceride, *TC* total cholesterol

* $p < 0.001$ versus CT diet + Sham

[a] $p < 0.001$ versus CT diet + HV

effect in mice fed an MCD diet for 8 weeks, whereas this effect was maintained in mice fed a CT diet for the same period (Fig. S4). Under conditions of choline deficiency-based NASH pathogenesis, vagus cholinergic signaling thus appears to have a greater impact during the early phase, before the attenuation of hepatic choline levels.

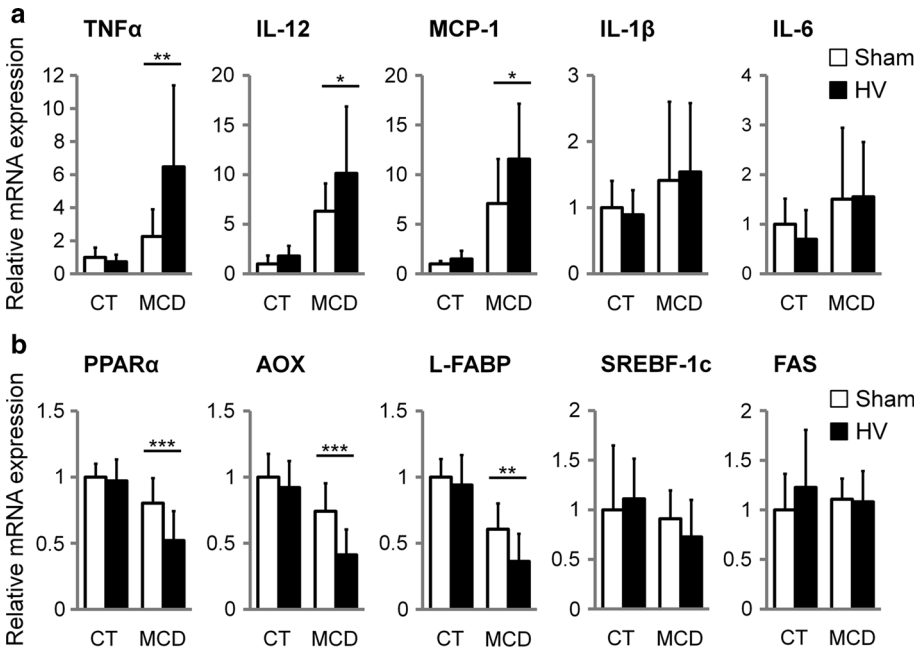

Fig. 2 Hepatic vagus denervation promotes NASH-associated inflammatory responses and abnormal lipid metabolism. **a**, **b** Hepatic mRNA expression of pro-inflammatory cytokine genes (**a**) and lipid metabolism-associated genes (**b**). Data were normalized to 18S. $n = 6$ per CT-diet group; $n = 12$ per MCD-diet group. Data represent the mean ± SD. $^{*}p < 0.05$; $^{**}p < 0.01$; $^{***}p < 0.001$

Hepatic vagus denervation promotes Kupffer cell activation in NASH

To assess the vagus-mediated anti-inflammatory effect during NASH development, we focused on the behavior of Kupffer cells, which play a key role in hepatic inflammatory responses. MCD dietary intake induced hepatic F4/80^{+} cell activation, which was morphologically characterized by cytoplasm enlargement and process expansion, and these changes were generally accompanied by NF-κB p65 phosphorylation and nuclear translocation (Fig. 3a). In the 1-week MCD diet model, HV promoted significant Kupffer cell activation, as represented by a larger area of F4/80^{+} cell infiltration as well as a higher proportion of phosphorylated p65 in these cells (Fig. 3b). Interestingly, the ratio of F4/80^{+} cell counts to total liver cells was unaffected by HV, and this ratio remained almost the same as that in the normal livers of CT diet-fed mice. This finding suggests that liver-resident macrophages, rather than those that secondarily migrate to the liver, are predominantly activated and modulated by hepatic vagus signaling during the early stages of NASH.

α7nAChR agonist suppresses the inflammatory response of Kupffer cells

We assessed the involvement of the vagus-mediated α7nAChR pathway in the regulation of Kupffer cell responses using primary Kupffer cell cultures. To mimic NASH pathogenesis in vitro, Kupffer cells were stimulated with palmitic acid, a lipotoxic free fatty acid, and LPS, a TLR agonist. Kupffer cells were activated, as evidenced by increased pro-inflammatory cytokine expression; specifically, palmitic acid and LPS stimulation synergistically upregulated TNFα and MCP-1 (Fig. 4a). The administration of an α7nAChR agonist effectively downregulated cytokine expression in Kupffer cells activated by palmitic acid and/or LPS (Fig. 4a). The α7nAChR agonist promoted STAT3 phosphorylation and suppressed p65 phosphorylation under TLR pathway stimulation by LPS (Fig. 4b). These modifications to STAT3 and NF-κB were involved downstream of the α7nAChR cascade and eventually led to the inhibition of pro-inflammatory cytokine transcription.

α7nAChR deficiency in Kupffer cells aggravates MCD diet-induced NASH

To assess the impact of cholinergic anti-inflammatory regulation via α7nAChR on Kupffer cells in vivo, we generated chimeric mice by transferring α7nAChR-deficient or WT BM cells into Kupffer cell-depleted WT recipients (Fig. 5a). Eight weeks after BM transplantation, mice were fed an MCD diet for 1 week. The reconstitution of Kupffer cells was assessed by immunohistochemical double staining for α7nAChR and F4/80; the absence of α7nAChR expression on Kupffer cells was verified in mice transplanted with α7nAChR-deficient BM cells (α7KO chimeric mice), whereas Kupffer cells in the mice transplanted with WT BM cells (WT chimeric mice) maintained α7nAChR expression (Fig. 5b). We further analyzed the efficacy of donor-derived Kupffer cell-reconstitution by depleting Kupffer cells and transplanting mice with green fluorescent protein-positive (GFP^{+}) BM cells to generate chimeric mice (Fig. S5a). The F4/80^{+} cells corresponded highly with GFP^{+} cells (GFP^{+} per F4/80^{+} cell count,

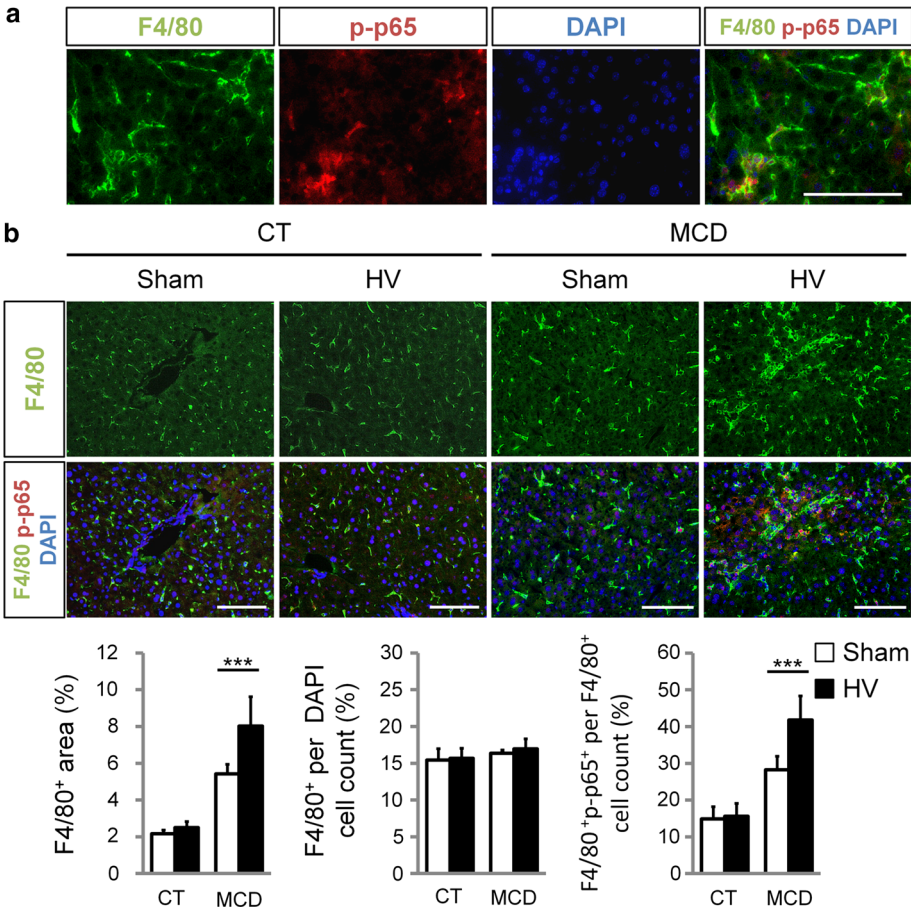

Fig. 3 Hepatic vagus denervation promotes Kupffer cell activation in NASH. **a**, **b** Immunohistochemical staining of liver sections for F4/80 and phospho-p65 (p-p65). **a** Liver sections from mice fed an MCD diet for 1 week. Original magnification ×200; scale bars, 100 μm. **b** *Top* Liver sections in sham-operated or HV mice fed an MCD diet for 1 week. *Bottom* Percentage of F4/80-stained area, F4/80$^+$ per total liver cell count, and both F4/80$^+$ and p-p65$^+$ per F4/80$^+$ cell count were measured. Original magnification ×100; scale bars, 100 μm. $n = 4$ per CT-diet group; $n = 6$ per MCD-diet group. Data represent the mean ± SD. ***$p < 0.001$

98.4 ± 0.5%; $n = 3$), indicating that Kupffer cells were precisely reconstituted with donor-derived cells. Conversely, the majority of intrahepatic GFP$^+$ BM-derived cells acquired not only F4/80 expression (F4/80$^+$ per GFP$^+$ cell count, 97.8 ± 0.2%; $n = 3$), but also the characteristic morphology and distribution of resident Kupffer cells (Fig. S5b).

The α7KO chimeric mice, in which Kupffer cells were reconstituted with an α7nAChR-deficient phenotype, developed more advanced steatohepatitis than the WT chimeric mice (Fig. 5c). Pathological steatosis, as well as lobular inflammation, was exacerbated in α7KO chimeric mice, as also indicated by lipid staining and the hepatic triglyceride content (Fig. 5d, e). The α7KO chimeric mice exhibited severe liver damage, with significantly higher serum transaminase levels (Fig. 5f).

α7nAChR deficiency in Kupffer cells promotes NASH-associated inflammatory responses and abnormal lipid metabolism

α7nAChR deficiency in Kupffer cells worsened the outcome of steatohepatitis. Thus, we assessed the activity of α7nAChR-deficient Kupffer cells in the liver tissue and its effect on the hepatic lipid metabolism. The Kupffer cells in α7KO chimeric mice were highly activated, as evidenced by a larger F4/80$^+$ area and a higher proportion of p65 phosphorylation. The ratio of F4/80$^+$ cell count to total liver cells did not change (Fig. 6a). The hepatic expression levels of the pro-inflammatory cytokines TNFα, IL-12, and MCP-1 were significantly upregulated in α7KO chimeric mice (Fig. 6b), consistent with the findings in the HV model. Regarding the modification of lipid metabolism, the expression of AOX, a regulator of the PPARα pathway, was downregulated. The expression levels of SREBF-1c and FAS, which are involved in fatty acids synthesis, were significantly increased (Fig. 6c). With respect to glucose metabolism, the hepatic expression of G6pc was significantly downregulated, whereas the serum glucose level remained unchanged (Fig. S6), suggesting that α7nAChR deficiency in Kupffer cells may be associated with the suppression of gluconeogenic gene expression.

Discussion

The vagus nerve is well known to play an essential role in maintaining metabolic homeostasis [31, 36–38]; it has also been reported to regulate innate immune responses and

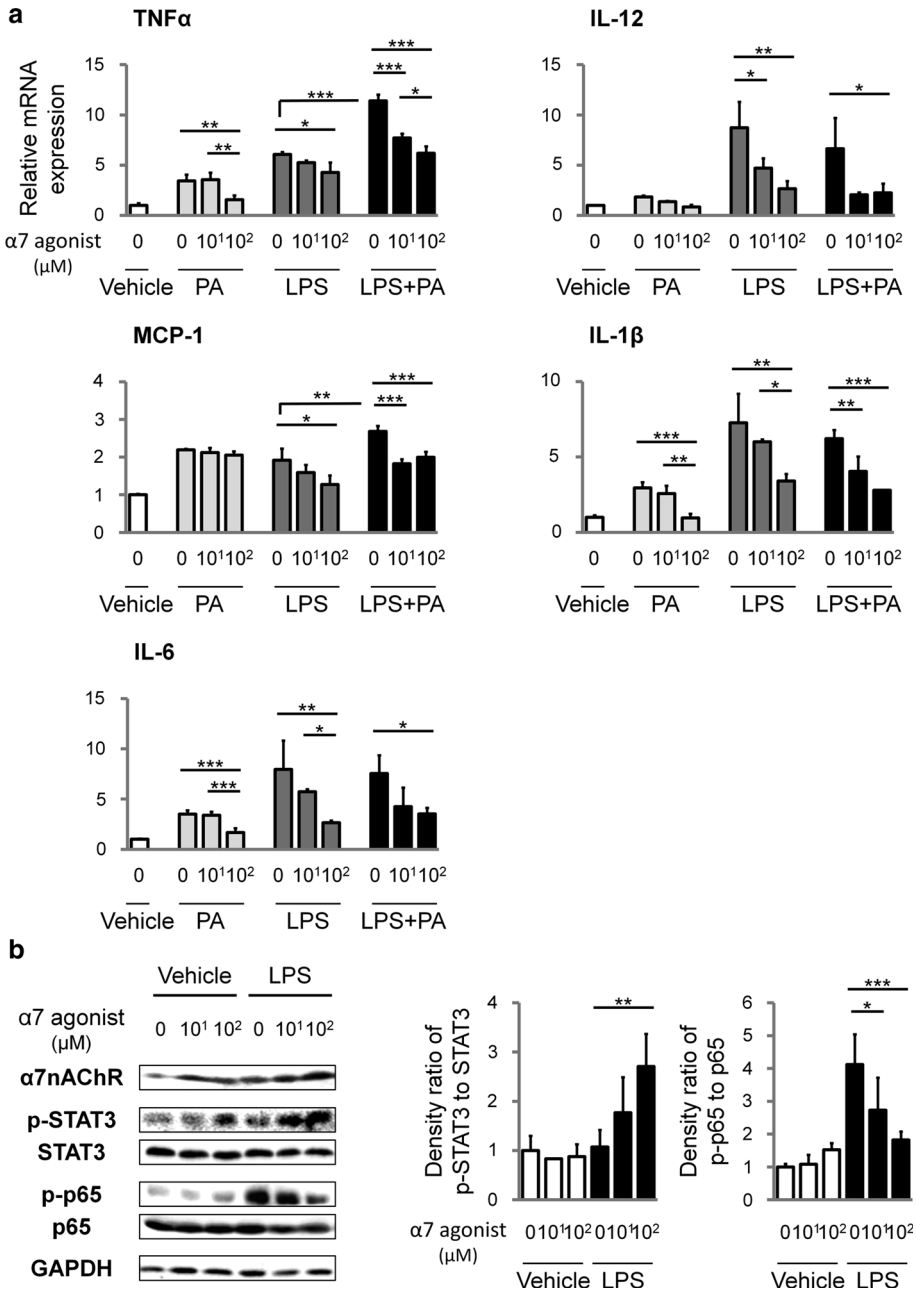

Fig. 4 α7nAChR agonist suppresses the inflammatory response in Kupffer cells. Primary Kupffer cells were treated with α7nAChR agonist under stimulation by LPS (1 ng/mL) and/or palmitic acid (400 μM). **a** mRNA expression of pro-inflammatory cytokine genes. Data were normalized to 18S. **b** Western blotting for α7nAChR, phospho-p65 (p-p65), p65, phospho-STAT3 (p-STAT3), or STAT3. Density ratios of bands of p-STAT3 to STAT3 and p-p65 to p65 were quantified. $n = 3$–5, each condition. Data represent the mean ± SD. $^{*}p < 0.05$; $^{**}p < 0.01$; $^{***}p < 0.001$

inflammation via the cholinergic stimulation of the α7nAChR. Decreased vagus nerve activity has been suggested to contribute to the obesity and metabolic syndrome-related complications resulting from chronic inflammation [30]. A recent study showed that central insulin action suppresses hepatic vagal activity, and the α7nAChR-mediated control of Kupffer cells is involved in the regulation of hepatic glucose production [39]. Given the vagus-mediated crosstalk between metabolism and immunity, the liver-specific activity of the vagus nerve is likely to affect the pathogenesis of NASH, a hepatic result of metabolic disorders and chronic inflammation. Moreover, α7nAChR stimulation has been suggested to exert a therapeutic effect on experimental NASH [40]; however, the mechanism underlying the α7nAChR-dependent control of hepatic inflammation and the effect of this control on hepatic lipid metabolism remain to be elucidated. We focused on the specific interaction between hepatic vagus cholinergic activity and the modulation of Kupffer cell-mediated inflammatory response via the α7nAChR pathway during the developmental phase of NASH, and our findings may provide a perspective for preventive and therapeutic strategies that compensate for vagus activity in patients with obesity and metabolic syndrome.

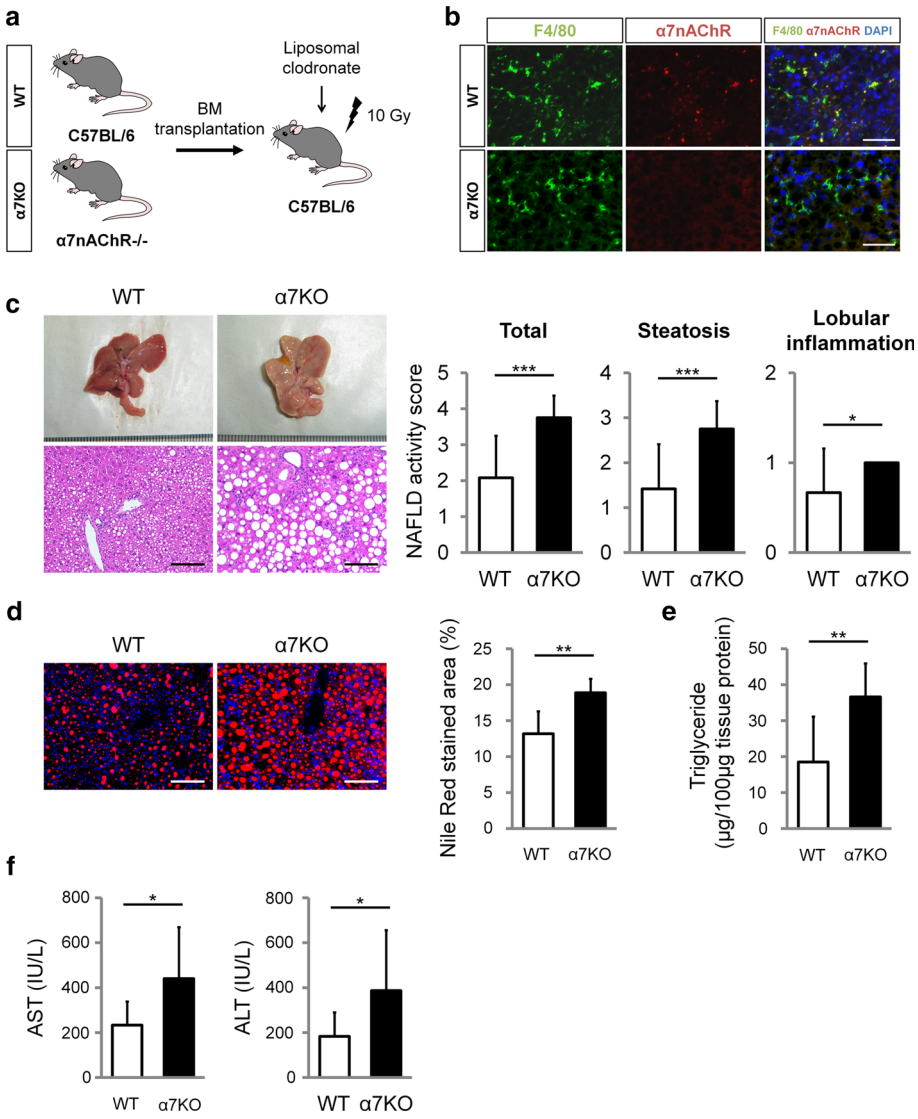

Fig. 5 α7nAChR deficiency in Kupffer cells aggravates MCD diet-induced NASH. Chimeric mice in which WT or α7KO BM cells were transplanted into WT recipients were fed an MCD diet for 1 week. **a** Procedure for generating chimeric mice. **b** Immunohistochemical staining of liver sections for F4/80 and α7nAChR. **c** *Left*: Macroscopic findings and hematoxylin-and-eosin-stained liver sections. *Right*: NAFLD activity score. **d** *Left* Nile Red staining of liver sections. *Right* Quantification of Nile Red-stained area. Original magnification ×100; scale bars, 100 μm. **e** Hepatic triglyceride content. **f** Serum aspartate aminotransferase (AST) and alanine aminotransferase (ALT) levels. $n = 6$ per group. Data represent the mean ± SD. $^{*}p < 0.05$; $^{**}p < 0.01$; $^{***}p < 0.001$

In the present study, hepatic vagus denervation aggravated MCD diet-induced steatohepatitis. As a result, Kupffer cells were highly activated, and a high proportion of p65 was phosphorylated, which upregulated the expression of pro-inflammatory cytokines, including TNFα and IL-12, and a chemokine associated with macrophage activation, MCP-1. Likewise, α7KO chimeric mice, in which Kupffer cells specifically lacked α7nAChR expression, developed severe steatohepatitis and highly activated Kupffer cells. Moreover, the α7nAChR agonist suppressed pro-inflammatory cytokine expression in primary Kupffer cells under LPS and palmitic acid stimulation. The STAT3 signaling pathway was involved downstream of the α7nAChR, resulting in the inhibition of NF-κB phosphorylation and subsequent pro-inflammatory cytokine expression. The results of the in vivo and in vitro studies indicate that hepatic vagus cholinergic signaling has an anti-inflammatory effect on Kupffer cells via an α7nAChR cascade during NASH pathogenesis.

In addition to the severity of inflammation, hepatic lipid accumulation was exacerbated in MCD diet-fed mice undergoing HV, and this change was accompanied by the downregulation of PPARα-pathway gene expression. The steatotic change was also accentuated in α7KO chimeric mice, in which all liver parenchymal cells except Kupffer cells were derived from the cells of the WT recipient. The modifications in lipid metabolism included the downregulation of AOX, which also occurred in the HV model, and the upregulation of SREBF-1c and its target FAS. The latter changes may reflect advanced metabolic disorder, partially due to the attenuated inhibition of SREBF-1c by the PPARα pathway [41, 42]. The severe inflammatory response induced by the selective blockage of the α7nAChR pathway in Kupffer cells secondarily affected lipid metabolism and steatotic change. In contrast, palmitic

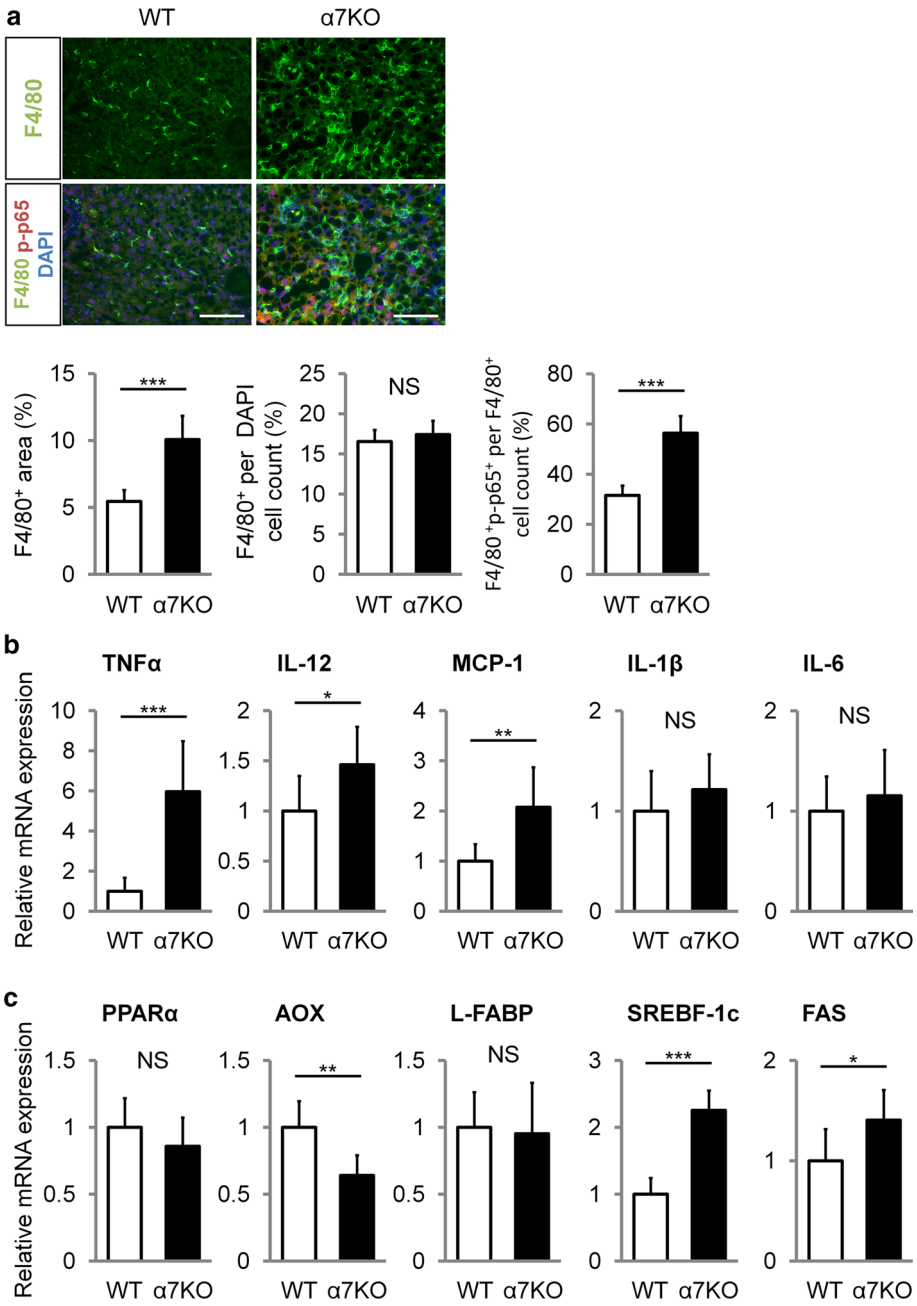

Fig. 6 α7nAChR deficiency in Kupffer cells promotes NASH-associated inflammatory responses and abnormal lipid metabolism. **a** *Top* Immunohistochemical staining of liver sections for F4/80 and phospho-p65 (p-p65). *Bottom* Percentage of F4/80-stained area, $F4/80^+$ per total liver cell count, and both $F4/80^+$ and $p\text{-}p65^+$ per $F4/80^+$ cell count were measured. Original magnification ×100; scale bars, 100 μm. **b**, **c** Hepatic mRNA expression of pro-inflammatory cytokine genes (**b**) and lipid metabolism-associated genes (**c**). Data were normalized to 18S. $n = 6$ per group. Data represent the mean ± SD. $^*p < 0.05$; $^{**}p < 0.01$; $^{***}p < 0.001$. *NS* not significant

acid administration induced inflammatory cytokine expression in primary Kupffer cells. Specifically, free fatty acids activate TLRs by binding fetuin-A contained in fetal bovine serum [43]. Stimulating Kupffer cells with palmitic acid and LPS synergistically upregulated TNFα and MCP-1, indicating that the lipotoxicity of free fatty acids as a consequence of hepatic lipid loading may also secondarily promote inflammation [44, 45]. Hepatic lipid metabolism and inflammatory responses closely interact with each other, which results in a vicious cycle of NASH progression that may be partially accelerated by decreased hepatic vagus activity and the subsequent attenuation of α7nAChR signaling in Kupffer cells. These findings may provide insight into a potential role for the vagus nerve in mediating crosstalk between metabolism and immunity.

The efferent vagus cholinergic signal was assumed to act directly on Kupffer cells and modulate their immune function. Hepatic vagus activity was suppressed after HV, as indicated by the significant decrease in hepatic acetylcholine content, resulting in severe hepatic inflammation and highly activated Kupffer cells. In addition to the direct mechanism of vagus-mediated anti-inflammatory signaling, a subset of memory $CD4^+$ T cells was reported to provide an endogenous source of acetylcholine that

stimulates the α7nAChR cascade [30, 46]. The function of acetylcholine-synthesizing T cells is modulated by efferent vagus nerve signaling, which is translated into noradrenergic splenic nerve activity in the spleen [46]. The selective denervation of the hepatic vagus nerve might not directly attenuate the activity of such a T cell population, as expected from the preserved acetylcholine level in the spleen. In the present study, we instead focused on the direct effect of hepatic vagus-mediated cholinergic signaling, but the interaction between liver-resident Kupffer cells and acetylcholine-producing T cells in NASH pathogenesis should be the subject of further study. The residual amount of hepatic acetylcholine that remained after denervation might partially derive from this T cell production or from hepatic vagus innervation that escaped surgical resection, e.g., innervation originating from the dorsal vagal trunk or other intrahepatic cholinergic neuronal networks. The detailed anatomical distributions of vagus nerve fibers, postganglionic neurons, and target cells in the liver remain controversial, making the assessment of their specific functions difficult. The selective blockage of target receptors in Kupffer cells using chimeric mice should help to confirm a one-to-one correspondence between vagus efferent signals and hepatic innate immune modulation.

The limitations of the present study are mainly associated with the MCD dietary model. In this experimental NASH model, hepatic steatosis and inflammation are certainly accentuated, while peripheral insulin resistance is preserved, and the mice do not develop obesity or metabolic syndrome but instead lose weight [47, 48]. The MCD dietary model does not strictly reproduce human NASH; specifically, it lacks extrahepatic effects, e.g., insulin resistance and gut- or adipose tissue-derived factors associated with obesity. Nevertheless, because we focused on liver-specific modulation by vagus efferent signals, this model might be well suited to assess the interaction between neural signals and NASH pathogenesis by minimizing such extrahepatic effects. Although the serum glucose levels were not affected in the MCD diet-fed HV mice or α7KO chimeric mice, the dysregulation of Kupffer cell activity by the attenuation of vagus-mediated cholinergic signaling resulted in significant downregulation of hepatic gluconeogenetic genes. These findings are consistent with those of a previous report on gluconeogenic suppression by α7nAChR-dependent Kupffer cell activation [39], and consequently may support the reproducibility and validity of the HV and the α7KO chimeric mice models used in the present study. Additionally, the relatively short-term induction of steatohepatitis by the MCD diet compared with other dietary models, e.g., a high-fat diet and a choline- and L-amino acid-deficient diet, might be advantageous for assessing the maximum influence of vagus activity before the effect of denervation declines. However, this model failed to assess the influence of the hepatic vagus nerve on the long-term consequences of NASH fibrogenesis because of the faint fibrogenic effect of the MCD diet and the reduced potency of denervation due to chronic choline deficiency, which may affect the baseline activity of the cholinergic signal. Based on the clinical features of choline deficiency in patients with NASH [49, 50], the impact of vagus-mediated cholinergic signaling might be strongest at the onset of NASH development, as we successfully demonstrated its effect on the inflammatory response during early-stage NASH.

In conclusion, the present study demonstrated that the hepatic vagus nerve plays a key role in regulating the inflammatory response in Kupffer cells via the α7nAChR pathway and eventually contributed to the suppression of NASH progression in its early phase. Our study may help elucidate the mechanisms by which the failure to modulate inflammatory events results in advanced disease in the NAFLD population.

Acknowledgements This work was supported by a Grant-in-Aid for Scientific Research from the Japan Society for the Promotion of Science (No. 15K15495), a grant from the Ministry of Education, Culture, Sports, Science and Technology of Japan (No. 26461909), and a grant from the Ministry of Health, Labor and Welfare of Japan.

Compliance with ethical standards

Conflict of interest The authors declare no conflicts of interest.

References

1. Fabbrini E, Sullivan S, Klein S. Obesity and nonalcoholic fatty liver disease: biochemical, metabolic, and clinical implications. Hepatology. 2010;51(2):679–89.
2. Hamaguchi M, Kojima T, Takeda N, et al. The metabolic syndrome as a predictor of nonalcoholic fatty liver disease. Ann Intern Med. 2005;143(10):722–8.
3. Marchesini G, Bugianesi E, Forlani G, et al. Nonalcoholic fatty liver, steatohepatitis, and the metabolic syndrome. Hepatology. 2003;37(4):917–23.
4. Starley BQ, Calcagno CJ, Harrison SA. Nonalcoholic fatty liver disease and hepatocellular carcinoma: a weighty connection. Hepatology. 2010;51(5):1820–32.
5. Matteoni CA, Younossi ZM, Gramlich T, et al. Nonalcoholic fatty liver disease: a spectrum of clinical and pathological severity. Gastroenterology. 1999;116(6):1413–9.
6. Day CP, James OF. Steatohepatitis: a tale of two "hits"? Gastroenterology. 1998;114(4):842–5.
7. Tilg H, Moschen AR. Evolution of inflammation in nonalcoholic fatty liver disease: the multiple parallel hits hypothesis. Hepatology. 2010;52(5):1836–46.
8. Li Z, Yang S, Lin H, et al. Probiotics and antibodies to TNF inhibit inflammatory activity and improve nonalcoholic fatty liver disease. Hepatology. 2003;37(2):343–50.
9. Lin HZ, Yang SQ, Chuckaree C, et al. Metformin reverses fatty liver disease in obese, leptin-deficient mice. Nat Med. 2000;6(9):998–1003.

10. Maher JJ, Leon P, Ryan JC. Beyond insulin resistance: innate immunity in nonalcoholic steatohepatitis. Hepatology. 2008;48(2):670–8.
11. Seki E, Brenner DA. Toll-like receptors and adaptor molecules in liver disease: update. Hepatology. 2008;48(1):322–35.
12. Miura K, Yang L, van Rooijen N, et al. Toll-like receptor 2 and palmitic acid cooperatively contribute to the development of nonalcoholic steatohepatitis through inflammasome activation in mice. Hepatology. 2013;57(2):577–89.
13. Rivera CA, Adegboyega P, van Rooijen N, et al. Toll-like receptor-4 signaling and Kupffer cells play pivotal roles in the pathogenesis of non-alcoholic steatohepatitis. J Hepatol. 2007;47(4):571–9.
14. Miura K, Kodama Y, Inokuchi S, et al. Toll-like receptor 9 promotes steatohepatitis by induction of interleukin-1beta in mice. Gastroenterology. 2010;139(1):323–34.
15. Leroux A, Ferrere G, Godie V, et al. Toxic lipids stored by Kupffer cells correlates with their pro-inflammatory phenotype at an early stage of steatohepatitis. J Hepatol. 2012;57(1):141–9.
16. Huang W, Metlakunta A, Dedousis N, et al. Depletion of liver Kupffer cells prevents the development of diet-induced hepatic steatosis and insulin resistance. Diabetes. 2010;59(2):347–57.
17. Kremer M, Thomas E, Milton RJ, et al. Kupffer cell and interleukin-12-dependent loss of natural killer T cells in hepatosteatosis. Hepatology. 2010;51(1):130–41.
18. Tosello-Trampont AC, Landes SG, Nguyen V, et al. Kuppfer cells trigger nonalcoholic steatohepatitis development in diet-induced mouse model through tumor necrosis factor-α production. J Biol Chem. 2012;287(48):40161–72.
19. Mandrekar P, Ambade A, Lim A, et al. An essential role for monocyte chemoattractant protein-1 in alcoholic liver injury: regulation of proinflammatory cytokines and hepatic steatosis in mice. Hepatology. 2011;54(6):2185–97.
20. Borovikova LV, Ivanova S, Zhang M, et al. Vagus nerve stimulation attenuates the systemic inflammatory response to endotoxin. Nature. 2000;405(6785):458–62.
21. Tracey KJ. The inflammatory reflex. Nature. 2002;420(6917):853–9.
22. Tracey KJ. Reflex control of immunity. Nat Rev Immunol. 2009;9(6):418–28.
23. Wang H, Yu M, Ochani M, et al. Nicotinic acetylcholine receptor alpha7 subunit is an essential regulator of inflammation. Nature. 2003;421(6921):384–8.
24. de Jonge WJ, van der Zanden EP, The FO, et al. Stimulation of the vagus nerve attenuates macrophage activation by activating the Jak2-STAT3 signaling pathway. Nat Immunol. 2005;6(8):844–51.
25. Parrish WR, Rosas-Ballina M, Gallowitsch-Puerta M, et al. Modulation of TNF release by choline requires alpha7 subunit nicotinic acetylcholine receptor-mediated signaling. Mol Med. 2008;14(9–10):567–74.
26. Guarini S, Altavilla D, Cainazzo MM, et al. Efferent vagal fibre stimulation blunts nuclear factor-kappaB activation and protects against hypovolemic hemorrhagic shock. Circulation. 2003;107(8):1189–94.
27. Rosas-Ballina M, Tracey KJ. Cholinergic control of inflammation. J Intern Med. 2009;265(6):663–79.
28. Wang X, Yang Z, Xue B, et al. Activation of the cholinergic antiinflammatory pathway ameliorates obesity-induced inflammation and insulin resistance. Endocrinology. 2011;152(3):836–46.
29. Satapathy SK, Ochani M, Dancho M, et al. Galantamine alleviates inflammation and other obesity-associated complications in high-fat diet-fed mice. Mol Med. 2011;17(7–8):599–606.
30. Pavlov VA, Tracey KJ. The vagus nerve and the inflammatory reflex—linking immunity and metabolism. Nat Rev Endocrinol. 2012;8(12):743–54.
31. Lam TK, Pocai A, Gutierrez-Juarez R, et al. Hypothalamic sensing of circulating fatty acids is required for glucose homeostasis. Nat Med. 2005;11(3):320–7.
32. Schneider CA, Rasband WS, Eliceiri KW. NIH Image to ImageJ: 25 years of image analysis. Nat Methods. 2012;9(7):671–5.
33. Kleiner DE, Brunt EM, Van Natta M, et al. Design and validation of a histological scoring system for nonalcoholic fatty liver disease. Hepatology. 2005;41(6):1313–21.
34. Folch J, Lees M, Sloane Stanley GH. A simple method for the isolation and purification of total lipides from animal tissues. J Biol Chem. 1957;226(1):497–509.
35. Tamaki N, Hatano E, Taura K, et al. CHOP deficiency attenuates cholestasis-induced liver fibrosis by reduction of hepatocyte injury. Am J Physiol Gastrointest Liver Physiol. 2008;294(2):G498–505.
36. Yi CX, la Fleur SE, Fliers E, et al. The role of the autonomic nervous liver innervation in the control of energy metabolism. Biochim Biophys Acta. 2010;1802(4):416–31.
37. Uno K, Katagiri H, Yamada T, et al. Neuronal pathway from the liver modulates energy expenditure and systemic insulin sensitivity. Science. 2006;312(5780):1656–9.
38. Pocai A, Obici S, Schwartz GJ, et al. A brain-liver circuit regulates glucose homeostasis. Cell Metab. 2005;1(1):53–61.
39. Kimura K, Tanida M, Nagata N, et al. Central insulin action activates Kupffer cells by suppressing hepatic vagal activation via the nicotinic alpha 7 acetylcholine receptor. Cell Rep. 2016;14(10):2362–74.
40. Zhou Z, Liu YC, Chen XM, et al. Treatment of experimental nonalcoholic steatohepatitis by targeting α7 nicotinic acetylcholine receptor-mediated inflammatory responses in mice. Mol Med Rep. 2015;12(5):6925–31.
41. Fernández-Alvarez A, Alvarez MS, Gonzalez R, et al. Human SREBP1c expression in liver is directly regulated by peroxisome proliferator-activated receptor alpha (PPARalpha). J Biol Chem. 2011;286(24):21466–77.
42. Yoshikawa T, Ide T, Shimano H, et al. Cross-talk between peroxisome proliferator-activated receptor (PPAR) alpha and liver X receptor (LXR) in nutritional regulation of fatty acid metabolism. I. PPARs suppress sterol regulatory element binding protein-1c promoter through inhibition of LXR signaling. Mol Endocrinol. 2003;17(7):1240–54.
43. Pal D, Dasgupta S, Kundu R, et al. Fetuin-A acts as an endogenous ligand of TLR4 to promote lipid-induced insulin resistance. Nat Med. 2012;18(8):1279–85.
44. Malhi H, Gores GJ. Molecular mechanisms of lipotoxicity in nonalcoholic fatty liver disease. Semin Liver Dis. 2008;28(4):360–9.
45. Alkhouri N, Dixon LJ, Feldstein AE. Lipotoxicity in nonalcoholic fatty liver disease: not all lipids are created equal. Expert Rev Gastroenterol Hepatol. 2009;3(4):445–51.
46. Rosas-Ballina M, Olofsson PS, Ochani M, et al. Acetylcholine-synthesizing T cells relay neural signals in a vagus nerve circuit. Science. 2011;334(6052):98–101.
47. Rinella ME, Elias MS, Smolak RR, et al. Mechanisms of hepatic steatosis in mice fed a lipogenic methionine choline-deficient diet. J Lipid Res. 2008;49(5):1068–76.
48. Hebbard L, George J. Animal models of nonalcoholic fatty liver disease. Nat Rev Gastroenterol Hepatol. 2011;8(1):35–44.
49. Guerrerio AL, Colvin RM, Schwartz AK, et al. Choline intake in a large cohort of patients with nonalcoholic fatty liver disease. Am J Clin Nutr. 2012;95(4):892–900.
50. Corbin KD, Zeisel SH. Choline metabolism provides novel insights into nonalcoholic fatty liver disease and its progression. Curr Opin Gastroenterol. 2012;28(2):159–65.